2019

The rapid chemically induced corrosion of concrete sewers at high H2S concentration

Xuan Li
University of Queensland

Liza O'Moore
University of Queensland

Yarong Song
University of Queensland

Philp Bond
University of Queensland

Zhiguo Yuan
University of Queensland

See next page for additional authors

The rapid chemically induced corrosion of concrete sewers at high H2S concentration

Abstract

Concrete corrosion in sewers is primarily caused by H2S in sewer atmosphere. H2S concentration can vary from several ppm to hundreds of ppm in real sewers. Our understanding of sewer corrosion has increased dramatically in recent years, however, there is limited knowledge of the concrete corrosion at high H2S levels. This study examined the corrosion development in sewers with high H2S concentrations. Fresh concrete coupons, manufactured according to sewer pipe standards, were exposed to corrosive conditions in a pilot-scale gravity sewer system with gaseous H2S at 1100 ± 100 ppm. The corrosion process was continuously monitored by measuring the surface pH, corrosion product composition, corrosion loss and the microbial community. The surface pH of concrete was reduced from 10.5 ± 0.3 to 3.1 ± 0.5 within 20 days and this coincided with a rapid corrosion rate of 3.5 ± 0.3 mm year −1. Microbial community analysis based on 16S rRNA gene sequencing indicated the absence of sulfide-oxidizing microorganisms in the corrosion layer. The chemical analysis of corrosion products supported the reaction of cement with sulfuric acid formed by the chemical oxidation of H2S. The rapid corrosion of concrete in the gravity pipe was confirmed to be caused by the chemical oxidation of hydrogen sulfide at high concentrations. This is in contrast to the conventional knowledge that is focused on microbially induced corrosion. This first-ever systematic investigation shows that chemically induced oxidation of H2S leads to the rapid corrosion of new concrete sewers within a few weeks. These findings contribute novel understanding of in-sewer corrosion processes and hold profound implications for sewer operation and corrosion management.

Keywords

h2sconcentration, induced, corrosion, concrete, rapid, sewers, chemically, high

Disciplines

Engineering | Science and Technology Studies

Publication Details

Li, X., O'Moore, L., Song, Y., Bond, P. L., Yuan, Z., Wilkie, S., Hanzic, L. & Jiang, G. (2019). The rapid chemically induced corrosion of concrete sewers at high H2S concentration. Water Research, 162 95-104.

Authors

Xuan Li, Liza O'Moore, Yarong Song, Philp Bond, Zhiguo Yuan, Simeon Wilkie, Lucija Hanzic, and Guangming Jiang

The Rapid Chemically Induced Corrosion of Concrete Sewers at High H_2S Concentration

Xuan Li [a], Liza O'Moore [b], Yarong Song [a], Philp. L. Bond [a], Zhiguo Yuan [a], Simeon Wilkie [a, c], Lucija Hanzic [b], Guangming Jiang [a, d, *]

[a] Advanced Water Management Centre, The University of Queensland, Australia

[b] School of Civil Engineering, The University of Queensland, Australia

[c] Division of Civil Engineering, University of Dundee, Scotland

[d] School of Civil, Mining and Environmental Engineering, University of Wollongong, Australia

XL: xuan.li@awmc.uq.edu.au; LO: l.omoore@uq.edu.au; YS: yarong.song @awmc.uq.edu.au; PB: phil.bond@uq.edu.au; SW: s.z.wilkie@dundee.ac.uk ; LH: l.hanzic@uq.edu.au; ZY: z.yuan@awmc.uq.edu.au

* Corresponding author. E-mail: g.jiang@awmc.uq.edu.au; gjiang@uow.edu.au; Tel.: +61 431 573 255.

Highlights:

- The first report of chemically induced concrete corrosion in sewers
- High concentration of H_2S can be chemically oxidized into sulfuric acid at sewer crown
- Sulfide oxidizing microorganisms were not participating in the rapid corrosion

Abstract:

Concrete corrosion in sewers is primarily caused by H_2S in sewer atmosphere. H_2S concentration can vary from several ppm to hundreds of ppm in real sewers. Our understanding of sewer corrosion has increased dramatically in recent years, however, there is limited knowledge of the concrete corrosion at high H_2S levels. This study examined the corrosion development in sewers with high H_2S concentrations. Fresh concrete coupons, manufactured according to sewer pipe standards, were exposed to corrosive conditions in a pilot-scale gravity sewer system with gaseous H_2S at 1100±100 ppm. The corrosion process was continuously monitored by measuring the surface pH, corrosion product composition, corrosion loss and the microbial community. The surface pH of concrete was reduced from 10.5 ± 0.3 to 3.1 ± 0.5 within 20 days and this coincided with a rapid corrosion rate of 3.5 ± 0.3 mm year $^{-1}$. Microbial community analysis based on 16S rRNA gene sequencing indicated the absence of sulfide-oxidizing microorganisms in the corrosion layer. The chemical analysis of corrosion products supported the reaction of cement with sulfuric acid formed by the chemical oxidation of H_2S. The rapid corrosion of concrete in the gravity pipe was confirmed to be caused by the chemical oxidation of hydrogen sulfide at high concentrations. This is in contrast to the conventional knowledge that is focused on microbially induced corrosion. This first-ever systematic investigation shows that chemically induced oxidation of H_2S leads to the rapid corrosion of new concrete sewers within a few weeks. These findings contribute novel understanding of in-sewer corrosion processes and hold profound implications for sewer operation and corrosion management.

Key words: Sewer, Corrosion, Concrete, Hydrogen sulfide, Chemically Induced Corrosion

1. Introduction

As one of the most critical components of the urban infrastructure in modern societies, sewer networks collect and transport sewage to treatment plants, preventing human exposure to unhygienic sewage and related sewage-borne diseases. The prevalence of concrete corrosion weakens the structural strength of sewers and leads to early collapse of pipes (Zhang et al. 2008). The damage inflicted on many sewer networks and the cost of preventive measures is a significant world-wide economic problem (Alexander et al. 2013, Jiang et al. 2016a, Jiang et al. 2015a). In addition to enormous sewer remediation expenditure, the structural failure also poses potential issues of odor emission and public safety (Jiang et al. 2017).

The corrosion of concrete pipes is mainly a result of hydrogen sulfide (H_2S). H_2S is formed by sulfate-reducing bacteria (SRB) in the anaerobic sewer biofilms/sediments. From the sewage, H_2S is emitted to the sewer air, part of which is absorbed/adsorbed into the moisture layer on the concrete walls exposed to air, here it is oxidized to sulfuric acid and causes corrosion (Li et al. 2017). H_2S is ubiquitous in sewer systems, although the concentrations differ temporally and spatially from a few ppm to several hundred ppm (Jiang et al. 2014, Wells and Melchers 2015).

Sewer concrete corrosion is a relatively slow process that may take years or decades to occur (Joseph et al. 2012). A three-stage concept proposed by Islander et al. (1991) is widely adopted to describe the corrosion development. In the initiation stage, the surface pH of the concrete is reduced from c.a.13 to c.a. 9 by carbonation and H_2S dissolution. This leads to the later stages where the pH of the concrete surface is conducive for microorganisms to colonize. Depending on the pH, both neutrophilic and acidophilic sulfide oxidizing microorganisms will biologically oxidize sulfur compounds to sulfuric acid. The reaction between cementitious material and sulfuric acid produces corrosion products like gypsum ($CaSO_4$), resulting in the structural

70 weakening of concrete sewers (Davis et al. 1998, Harrison Jr 1984, Islander et al. 1991, Nica
71 et al. 2000, Parker 1947). Since the biological oxidation rate is much higher than the chemical
72 oxidation rate, microbial induced sulfuric acid production is regarded as the main cause for the
73 sewer concrete corrosion (Hvitved-Jacobsen et al. 2013).

74 Current strategies for controlling sewer corrosion are targeted to: (1) prevent H_2S production
75 and its partition from the sewer liquid phase through the dosing of antimicrobials, iron salts,
76 pH elevating compounds and oxidants to the sewage; (2) reduce the H_2S concentration in sewer
77 air through forced ventilation; (3) applying surface treatment on concrete sewers (Jiang et al.
78 2015a). Corrosion resistant materials like antimicrobials, silver-loaded zeolite, and polymers
79 coatings are widely used to mitigate the corrosion of sewers (Berndt 2011, De Muynck et al.
80 2009, Haile and Nakhla 2010, Sun et al. 2015).

81 With the increased use of corrosion-resistant materials and surface treatments in sewers,
82 instead of reacting with concrete, the H_2S in sewer air can accumulate to very high
83 concentrations. In real sewers, H_2S concentrations of over 800 ppm are observed in a gravity
84 pipe (Wells and Melchers 2015). Furthermore, various factors such as high wastewater sulfate
85 concentrations, and extended hydraulic retention times can lead to high sewer H_2S
86 concentrations (Lahav et al. 2004, Sharma et al. 2008).

87 To date, microbially induced sulfuric acid generation from H_2S is considered as the major
88 contributing cause of sewer mass loss and structure failure. However, elevated H_2S
89 concentrations in sewers might result in changed corrosion mechanisms and processes. In
90 particular, the chemical oxidation rate of sulfide would be greatly increased, due to the
91 reaction's n^{th} order kinetics (n = 0.90–1.38) (Chen and Morris 1972, Haaning Nielsen et al.
92 2004). Considering the relative slow growth of sulfide oxidizing microorganisms and the
93 potential toxicity of H_2S, the chemical oxidation could play a more important role than the
94 microbial oxidation to the corrosion under high sewer H_2S conditions.

95 The kinetics of the chemical oxidation of H_2S on the concrete surface has received limited
96 attention (Æsøy et al. 2002). The pathway of microbial oxidation of H_2S has been studied
97 previously and elemental sulfur, thiosulfate, and sulfate are reported as the possible oxidation
98 products/intermediates (Li et al. 2017, Nica et al. 2000, Parker 1945a). Very few studies have
99 investigated the concrete corrosion induced by chemical sulfide oxidation. H_2S absorption and
100 oxidation on corroding concrete surfaces was examined at peak concentrations around 1000
101 ppm (Vollertsen et al. 2008). Here they reported that the H_2S oxidation rate was as high as 1
102 mg S m^{-2} s^{-1} and it followed the n^{th} order kinetics (n = 0.45–0.75). However, the study did not
103 differentiate whether the rapid sulfide oxidation was chemical or biological. Another study has
104 investigated the abiotic and biotic oxidation of hydrogen sulfide in in an acidic solution
105 containing active concrete corrosion products {Jensen, 2009 #246}. In this study, the abiotic
106 oxidation was much slower compared with the biotic oxidation. But the oxidation products of
107 sulfide were not examined for abiotic oxidation and the abiotic kinetics were limited to acidic
108 solution containing corrosion layer.

109 Unlike in concrete systems, numerous investigations regarding the chemical sulfide oxidation
110 have been carried out in water, where pH shows significant impact on the oxidation process.
111 In acidic solutions, the chemical oxidation rate is slow at pH < 6 and once the pH increases
112 through 7 to 11, the oxidation rate increases greatly (Chen and Morris 1972). On concrete
113 surface, the condensation water layer provides the essential medium for the chemical and
114 biological sulfide oxidation reactions. It is thus possible that the newly manufactured concrete
115 sewers, that will have high surface pH, are susceptible to the corrosion caused by chemical
116 oxidation of sulfide at high H_2S concentrations.

117 Thus, at high H_2S concentrations, the three-stage concept of corrosion development for newly
118 manufactured concrete sewers, it is likely very important to consider the contribution of
119 chemical sulfide oxidation prior to the occurrence and contribution of microbially induced

corrosion. To our knowledge, no systematic investigation has been conducted to monitor the corrosion under high H_2S concentrations and to determine the corrosion behavior, including corrosion rate and products, of newly constructed concrete sewers.

In this study, the development of corrosion was studied in detail on concrete coupons exposed in a pilot sewer system with high H_2S concentrations (1100±100 ppm). The corrosion rate, processes and products were determined by measuring the changes of concrete properties such as surface pH, sulfide oxidation products, microbial communities on the surface and mineralogy. Batch tests were then performed to determine the sulfide oxidation kinetics in the presence of fresh concrete powder or corrosion products. The knowledge obtained regarding the chemically induced corrosion of concrete has important practical implications for sewer operation, maintenance and management.

2. Materials and methods

2.1. Concrete mix design and property

Concrete coupons were prepared according to the mix design (**Table 1)** in compliance with the Australian standard (Standard AS2972) (2010). The cement (General Blended cement, Cement Australia Builders Cement) used nominally contains up to 25% fly ash. Four types of aggregates were used, including crushed aggregate (10 mm) with nominal maximum size of 10 mm; crushed manufactured sand (MS); natural river sand (RS) and natural fine sand (FS). For the better workability and moderate slump retention, super plasticizer (MasterGlenium SKY 8700, BASF, Australia) was also added (Table 1).

Table 1. Concrete coupon mix design and properties

W/C[a]	Constituents [a], (*kg m^{-3}*)		Compressive strength *(MPa)*
	Cement (GB)	Aggregates	

		10mm	MS	RS	FS	TOTAL	Super plasticiser	
0.40	420	753	376	471	282	1882	4.2	63

[a] Constituents are given as mass needed to form 1 m^3 of concrete

[b] W/C: water/cement mass ratio

Properties of the concrete including compressive strength, density, shrinkage, slump and apparent volume of permeable voids were measured in accordance with the AS 1012.9 (Australian Standard 1986) for the requirements of sewer pipe (Table 1, Table S1). The acid neutralization capacity (ANC) was determined by titrating a given mass of the concrete against various quantities of 0.4 M sulfuric acid using the methods adapted from (Sun et al. 2014) and as described in **section 1.2-SI**.

Concrete coupons were cast with dimensions of 100 mm (length) ×70 mm (width) ×50 mm (thickness). The coupons were cured in moist air for 24 h and then cured in lime-saturated water for 28 days. After curing, the coupons were dried in an oven (Thermotec 2000, Contherm) at 60 ºC for 3 days to achieve similar and stable initial water content (Joseph et al., 2010). Two dried coupons were then embedded as a pair in a stainless steel frame, providing a reference point for determining the change in thickness due to corrosion (Jiang et al., 2014). And then coupons was enclosed with one surface exposed for each coupon using epoxy (FGI R180 epoxy & H180 hardener).

2.2. Corrosion tests in the pilot-scale gravity sewer pipe

The pilot-scale gravity sewer pipe (225 mm ID PVC pipes), located in the Luggage Point Wastewater Treatment Plant (WWTP, Brisbane, Australia) (Figure 1), had a total workable length of 300 meters with an overall slope at 0.56%. Raw wastewater of the WWTP influent

was fed to the gravity pipe continuously at 100 L min^{-1}. The wastewater contained dissolved sulfide at 27.2± 0.5 mg-S L^{-1}, sulfate at 15-20 mg-S L^{-1}, and chemical oxygen demand (COD) at 550–620 mg L^{-1}. The pilot sewer system was controlled by a programmable logic controller (PLC), and the operation state was manipulated using the Lab-View (Lab-View 2014, Real Time) (Song et al. 2018a).

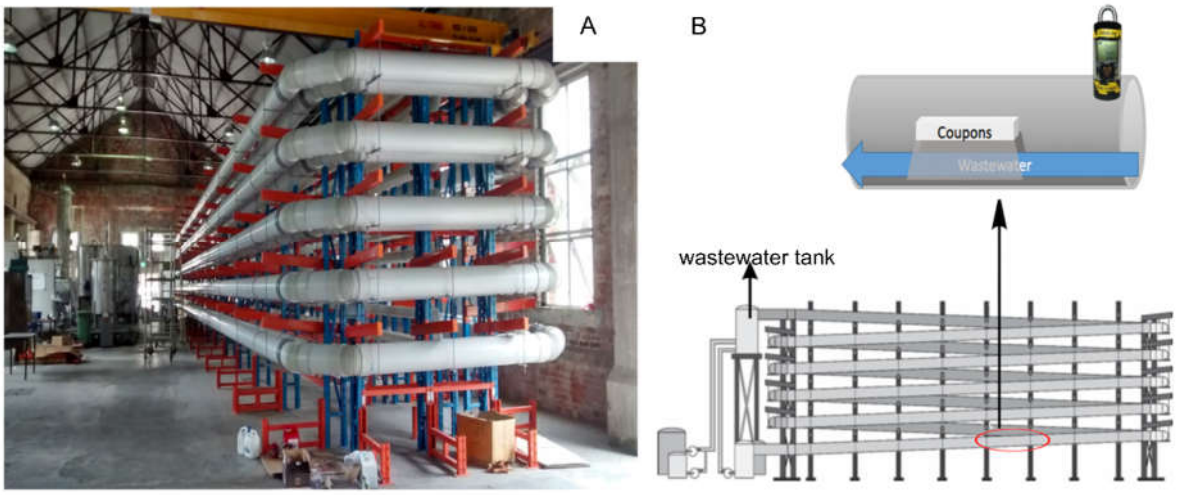

Figure 1. Photo of the pilot-scale gravity sewer system (A) and a schematic diagram of the pipe and the coupon installment for corrosion tests (B)

Four concrete coupons, enclosed in stainless-steel frames, were installed in the gas-phase of the gravity sewer pipe, at about 250 meters away from the sewer inlet. The coupons were placed on a plastic shelf inside the pipe so that the exposed surface was facing downwards, approximately 110 mm above the sewage level (Figure 1). This coupon arrangement simulated the sewer pipe crown, a location which is reported to be highly susceptible to corrosion damage (Islander et al. 1991). A H_2S sensor (App-Tek OdaLog® Logger L2, detection range of 0-2000 ppm) was employed for the continuous monitoring of gaseous H_2S and temperature in the pipe at the coupon location. The relative humidity (RH) was measured weekly using a hand-held humidity meter (HM70, Vaisala, Australia). After 20 days of exposure the four concrete

178 coupons were retrieved for detailed chemical and biological analysis as described in the
179 following sections.

180 *2.3. Sulfide oxidation rate (SOR) of coupons*

181 To determine sulfide oxidation rates (SOR), sulfide uptake rates (SUR) of two coupons under
182 500-1500 ppm H_2S were measured after 20 days' exposure in the sewer pipe using the method
183 described in Sun et al. (2014). Briefly, coupons retrieved from the pilot sewer were stored in
184 a chamber with 100% humidity until placed into the H_2S uptake reactor where the relative
185 humidity was controlled at 100%. To measure the SUR of each target concentration (i.e. C_i,
186 ppm), H_2S gas was generated in a bottle and injected into the reactor to achieve a gaseous
187 concentration 20 ppm higher than the target concentration (i.e. $C_i + 20$, ppm). The H_2S level in
188 the reactor was then monitored continuously using a H_2S detector (App-Tek OdaLog® Logger
189 L2, detection range of 0-2000 ppm). The average SUR of the coupon at each target level was
190 calculated from 3 to 5 replicate measurements using the monitored H_2S profiles (Sun et al.,
191 2014). H_2S uptake data of the concrete coupons were determined in the presence of either air
192 (SUR_{Air}) or nitrogen gas to exclude oxidation reactions ($SUR_{Nitrogen}$). Based on these two SUR
193 measurements, the sulfide oxidation rate (SOR) of a concrete coupon was defined as:

194 $$SOR = SUR_{Air} - SUR_{Nitrogen} \quad (1)$$

195 To determine the chemical oxidation rate of sulfide, the surface of two coupons were sprayed
196 with 50 ml 70% ethanol and then left to dry in a laminar flow sterile hood for 2 hours (Gu et
197 al. 1998). The sterilized samples were then equilibrated with 100% humidity until a constant
198 weight and then the SOR of the sterilized coupons was measured in the reactor as described
199 above using a H_2S detector (App-Tek OdaLog® Logger L2, detection range of 0-200 ppm).

200 *2.4. Analysis of corrosion on concrete coupons*

The concrete surface pH of each coupon was determined by a flat surface pH electrode (RapidRH® potable pH kit, Wagner) (Sun et al., 2014). Four independent measurements at different locations on the same coupon were used to calculate the average value.

The corrosion products on the surface of the exposed concrete coupons were then sub-sampled for the analysis of sulfur compounds and microbial communities. For soluble sulfate measurement, samples from a known surface area (4 independent locations) of each coupon was scraped using a clean scalpel blade, dispersed into sulfide anti-oxidant buffer solution and then measured using ion chromatography (Dionex ICS-2000)(Keller-Lehmann et al. 2006). For elemental sulfur analysis, corrosion products collected from known surface area (4 independent locations) were treated to convert elemental sulfur to thiosulfate, which was then determined using ion chromatography (Dionex ICS-2000) (Jiang et al. 2009)

For DNA extraction, in order to get sufficient amount of sample, all the corrosion products, except used for sulfur compounds measurements, from four coupons were collected with a sterile surgical scalpel into a sterile 50 mL polypropylene falcon tube. The products were mixed, separated into duplicate samples and stored at 4 °C for less than 24 h. Wastewater samples were taken directly from the gravity pipe through sampling ports and stored at 4 °C for less than 24 h. The cells were separated from the corrosion products using a sucrose density gradient and DNA of the corrosion products and wastewater samples were extracted using the Fast DNA™ SPIN Kit for Soil (MP Biomedicals, CA, USA), as previously described (Jiang et al. 2016b). To perform 16S rRNA gene amplicon sequencing (Illumina),extracted DNA samples were provided to the Australia Center for Ecogenomics (ACE, Brisbane, Australia). The extracted 16S rRNA gene was amplified using the universal primer set 926F (5'-AAACTYAAAKGAATTGACGG-3') and 1392R (5'-ACGGGCGGTGTGTRC-3'). The resulting PCR amplicons were purified using Agencourt AMPure XP beads (Beckman Coulter). Then the purified DNA was indexed using the Illumina Nextera XT 384 sample Index Kit A-

D (Illumina FC-131-1002) in standard PCR conditions with Q5 Hot Start High-Fidelity2X Master Mix. The indexed amplicons were pooled together in equimolar concentrations and sequenced on MiSeq Sequencing System (Illumina) at ACE according to manufacturer's protocol.

Raw sequencing data were quality-filtered and demultiplexed using Trimmomatic, with poor-quality sequences trimmed and removed. Subsequently, high-quality sequences at 97% similarity were clustered into operational taxonomic units (OTUs) using QIIME with default parameters, and representative OTU sequences were taxonomically BLASTed against the Greengenes 16S rRNA database. Finally, an OTU table consisting of the taxonomic classification and OTU representative sequences was produced.

To examine the chemistry and mineralogy of corrosion products formed on the concrete surface, small slices of exposed surface from each coupon (four in total) were carefully removed using a chisel, and dried in a vacuum oven (SEMSA OVEN 718) at 60 ℃ for 8 h. The dried samples were then coated twice by a carbon coater (Quorum Q150T, UK), following the three heavy-burst model to obtain the carbon thickness of 30-40 nm. Coated samples were analyzed by the scanning electron microscopy (SEM) (JEOL JSM-6610, America) equipped with a detector (Oxford 50mm2 X-Max SDD x-ray) that enables simultaneous imaging and elemental analysis at high count rates with 125 eV energy resolutions. The EDAX software (EDAX, AMETEK Inc) was utilized, at a frame resolution of 1024×800, with a dwell time of 200 s/frame, to collect 16 frames for each region of interest. The locations for spot analyses were not random, but chosen by examining the BSE (Backscattered electron) image, which was typically used to identify the boundaries of mineral phases (Song et al. 2018b).

After all the measurements mentioned above, the exposed surfaces of concrete coupons were washed using a high-pressure washer (Karcher K 5.20 M). The corrosion loss from the surface

of each coupon was calculated based on the point mesh generated before and after exposure, using the photogrammetry approach (Jiang et al. 2015b, Wells et al. 2009).

2.5. Batch tests: sulfide oxidation in the presence of concrete and corrosion products

Batch tests were performed to determine the oxidation of hydrogen sulfide by oxygen in the presence of crushed powder from fresh concrete or corrosion products based on a modified method (Jensen et al. 2011). The batch tests were conducted in a glass reactor with 800 mL working volume at 24 ± 0.5 ºC (Figure S1). A pH sensor (pH 150, Oakton) and a dissolved oxygen (DO) sensor (LDO101, HQ40d, Hach) were mounted to the reactor and sealed with Teflon tape (Oxygen tape, Unasco Pty Ltd, Sydney, Australia). The solution was mixed at 100 rpm using a magnetic stirrer (Heidolph MR3000). A 50 mL syringe filled with the testing solution was used as a sample replacer to avoid headspace or negative pressure inside the reactor during sampling.

For fresh concrete powder, samples cut from the center of new concrete were disaggregated in an agate mill, then the aggregate free material was crushed to <0.5 mm particles and then mixed together with the aggregates collected from disaggregation process. Corrosion products were collected using a sterile surgical scalpel from a corroding concrete coupon, which was partially submerged in wastewater in the pilot-scale gravity pipe (Figure 1) for one month. The corrosion products were autoclaved at 120°C for 20 minutes, and then cool down to 20 °C. For each test, either crushed fresh concrete powders (20 g) or autoclaved corrosion products (10 g) were transferred into the reactor with aerated milli-Q water.

Duplicate tests were carried out with no headspace in the reactor. At the beginning of each test, the sulfide stock solution (about 300 mg-S L^{-1}) was prepared using $Na_2S{\cdot}9H_2O$. The sulfide was added to the reactor to achieve 5.0-6.5 mg-S L^{-1}, which corresponded to an equilibrium concentration of gaseous H_2S at 400–1000 ppm (pH 2-10) (Jensen et al. 2011). Liquid samples

were taken at 15 minute intervals during the first hour and then every 1-hour over 4 hours for the analysis of inorganic sulfur compounds using ion chromatography (Dionex ICS-2000)(Keller-Lehmann et al. 2006).

3. Results and discussion

3.1. Corrosion of concrete coupons exposed in the gravity sewer

3.1.1 Visual inspection, surface pH and corrosion rate

During the exposure period, the gaseous H_2S concentration inside the pipe was at 1100±100 ppm, the temperature was 21.5± 2.4 ºC, and the relative humidity was 95.7 ± 3.0%. This level of H_2S inside the pipe represented high level hot spots that occur in sewers. The high level also facilitated the observation of measurable corrosion within a reasonable timeframe (i.e. exposure time of several weeks).

From visual inspection, before exposure, the grayish surface of all four coupons was smooth and firm (Figure 2). After 20 days, the color of entire surface became darker and obvious corrosion products were observed at the edge of coupons (Figure 2). The corrosion products were a light yellow color, expansive and loose. This is similar to typical corrosion products formed due to microbial induced corrosion (Cayford 2012). The middle part of each coupon was still sound with some dark spots observed from visual inspection. Likely the darks spots were attributed to the leaching of ferruginous components of aggregates (Jana and Lewis 2005).

Figure 2. The surface conditions of the four concrete coupons before exposure (the first row), and after 20-days exposure (the second row).

Regional differences regarding pH was also observed on these coupons. The surface pH of coupons reduced from 10.5±0.3 to 3.1±0.5 at the edge and to 7.7±0.1 in the middle parts after 20 days of exposure in the pipe. Surface pH is usually regarded as a good indicator of corrosion development and mass loss of concrete, as the alkalinity of the exposed concrete surface is consumed by direct or indirect reaction with H_2S in the sewer atmosphere. In a real sewer with 423 ppm of H_2S, the surface pH dropped from c.a. 10 to c.a. 7 in 6 months then further reduced to c.a. 4 in 20 months (Wells and Melchers 2015). Another lab study found that the surface pH was reduced from c.a. 10 to c.a. 7 and c.a. 4 in 6 months and 24 months exposure to 50 ppm of H_2S, respectively (Jiang et al. 2015b). In comparison, the reduction of surface pH on both the middle and edge parts of the concrete coupons were much faster in this study. The pH reduction of concrete would eventually lead to the loss of concrete (Islander et al. 1991).

The average corrosion rate was determined from the four coupons as 3.5± 0.3 mm $year^{-1}$ during the 20 day exposure. Consistent with the pH and visual inspection, the corrosion rate is not uniform on the surface of each coupon. The corrosion on about 40-60% area of each coupon was observed to be insignificant (Figure 3). Whereas, several peaks of higher corrosion rates

311 on less than 10% area of each coupon, were observed at around 9 mm year^{-1}, 2-5 mm year^{-1},
312 around 7 mm year^{-1} and around 5 mm year^{-1} for coupon I, II, III and IV, respectively (Figure
313 3). These higher corrosion rates were observed on areas along the edges of the coupons. As a
314 combination of cement, water, aggregates and other admixtures, concrete is not a homogenous
315 material. The structure of concrete around the edge is likely to be less sound due to the density
316 gradient of cement and aggregates, in comparison to the middle parts of the coupons.
317 Additionally, areas along the coupon edges on the surface were likely subjected to corrosion
318 attack from both the exposure surface and from the sides of exposure surfaces.

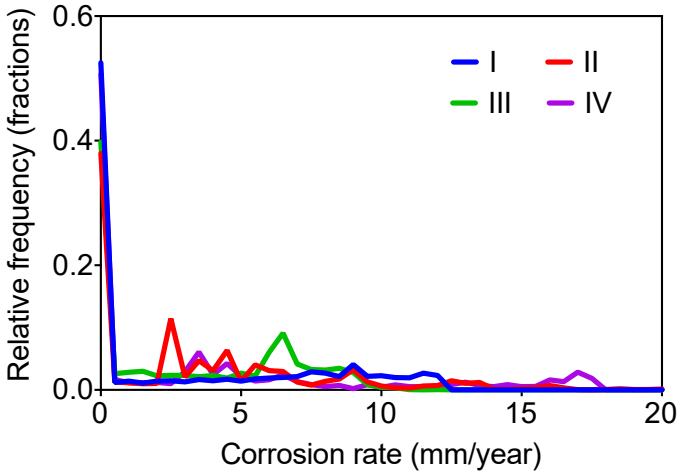

319

320 **Figure 3.** Relative frequency distribution of corrosion rates on the exposed surface of the four
321 coupons (I, II, III and IV)

322

323 The average corrosion rate observed was similar to the rates detected on pipes subjected to
324 corrosion in the USA, and higher than the rate of a sewer pipe with 12 years exposure, that is
325 reportedly due to microbial induced corrosion (Zhang et al. 2008, Mori et al. 1991). The
326 coupons used in this study were produced from fly ash blended concrete. Fly ash blended
327 concretes are reported to be resistant to sulfide-oxidizing bacteria and have lower corrosion
328 rates (1.0–1.3 mm year^{-1})). The corrosion rate detected in this study, especially on the coupon
329 edge areas, was higher than that previously reported for fly ash blended concrete and for most

330 sewer corrosion studies (Zhang et al. 2008, Mori et al. 1991). Furthermore, in studies of
331 microbial induced concrete corrosion, the corrosion rates are usually reported after an initiation
332 period. The initiation of corrosion on new concrete was conventionally considered as a slow
333 process that takes several years or decades (Joseph et al. 2012). For example, corrosion loss
334 was only observed after 12-months exposure in a real sewer with H_2S concentrations as high
335 as 423 ppm and after 34-months exposure in a laboratory corrosion chamber with 50 ppm H_2S
336 (Jiang et al. 2015b, Wells and Melchers 2015). The fast corrosion that developed within 20
337 days in this study was different from all the previous reports.

338 The visual inspections, pH reduction and the determined corrosion rates confirmed the rapid
339 development of corrosion on the coupon surface. This differs to what is previously reported
340 and this rapid corrosion was very likely due to the extremely high concentration of H_2S, which
341 facilitated the chemical oxidation of sulfide.

342 3.1.2 Corrosion product characteristics

343 The microstructure analysis using SEM revealed considerable mineralogical changes on the
344 coupon surface. Angular crystal formations were observed to be sulfur-containing corrosion
345 products (**Figure 4A**, **Figure S2)** (Cayford 2012). These corrosion products were either loosely
346 scattered on fly ash (region 1, Figure 4A) (Kutchko and Kim 2006), or piled up on a cement
347 matrix (region 2 and 3, Figure 4A). Hexagonal formations (region 3, Figure 4A) and a
348 collection of amorphous particles (region 2, Figure 4A) were observed, and these were typical
349 of hydration products of cement, cement-calcium hydroxide, and calcium silicate hydrate
350 (Franus et al. 2015). Lesser amounts of those hydration products were observed in comparison
351 to corrosion products, which suggests that alkalinity loss occurred due to the corrosion process.
352 Similar microstructure was observed for all these four coupons (i.e. coupon I, II, III and IV)
353 (Figure S2). In microbially induced concrete corrosion, microbial cells are detected by SEM

as small elongated shapes in the corrosion layer (Cayford et al. 2017). In this study, no evidence of microbes was found in the corrosion layer (Figure 4A, Figure S2).

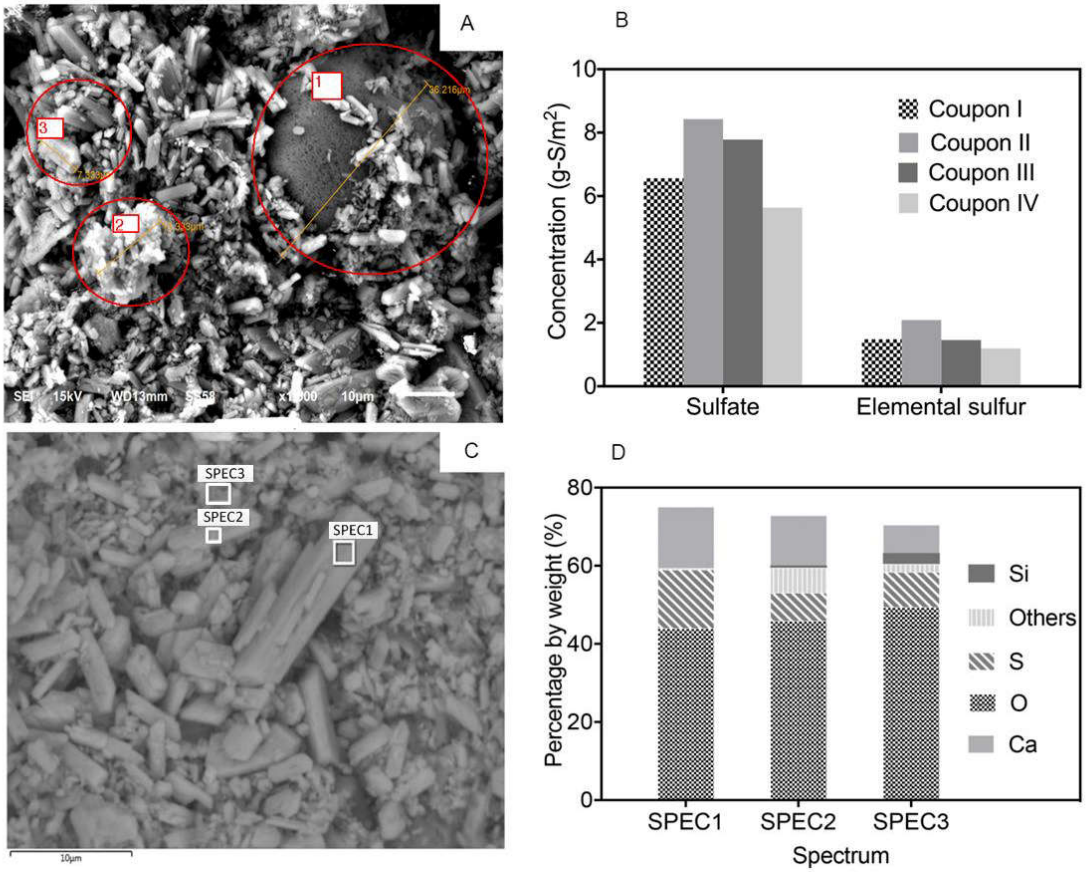

Figure 4. A SEM image of corrosion products on the surface of coupon I after the 20-day exposure in the pilot gravity sewer pipe (A), sulfur species in the corrosion products (B), BSE image indicating the regions on the coupon I surface selected for EDS analysis, shown as SPEC 1, 2 and 3 (C), and the percentage of elements by weight, except the coating material, of SPEC 1, 2 and 3 (D)

Based on the different regional brightness in BSE images (Figure 4C, Figure S2), the major elements, minus the coating material, were detected at the typical spots for each coupon (i.e. SPEC1, 2, 3) by EDS analysis (Figure 4C, D). The corrosion products, formed in the angular shapes (SPEC 1, Figure 4 C), mainly consisted O, Ca and S with the atomic ratio of 6.3: 0.9: 1.0 (O: Ca: S). This suggests that the angular crystal corrosion products is mainly gypsum

367 ($CaSO_4 \cdot 2H_2O$), a typical corrosion product in microbial induced concrete corrosion (Grengg
368 et al. 2015, Gutierrez-Padilla and Dolores 2007). Similar to SEM images, the corrosion
369 products were piled up on calcium hydroxide (hexagonal formations) in SPEC 2 and calcium
370 silicate hydrate (a collection of amorphous particles) in SPEC 3 (Figure 4 C), where the
371 calculated atomic ratios were 7.1: 0.8: 1.0 (O: Ca: S) and 10.1: 0.7: 1.0: 0.5 (O: Ca: S: Si),
372 respectively. Although the atomic ratio varied depending on the associated hydration products,
373 the O/S ratio, and the soluble sulfur species analysis of the corrosion products collected from
374 each coupon surface, further confirmed that sulfate was the dominant product of the H_2S
375 oxidation with some elemental sulfur present in the corrosion product (Figure 4B).

376 Previously, elemental sulfur was the main product in the initiation stage in laboratory chamber
377 experiments, where it was reported that the abiotic process of concrete corrosion mainly
378 occurred (Jiang et al. 2015b, Joseph et al. 2012). Sulfate was only detected in corrosion
379 products after twelve-month exposure in a laboratory chamber with 50 ppm of gaseous H_2S
380 (Jiang et al. 2015b, Joseph et al. 2012). During the initiation stage, the maximum amount of
381 sulfate was reposted as 2.2 g m^{-2} after twelve months exposure, while the levels of elemental
382 sulfur were more than an order of magnitude higher (Joseph et al. 2012). In contrast, the sulfate
383 content of corrosion products on the whole coupon surface in this study were 2-3 times higher
384 than elemental sulfur and were two times higher than the maximum concentration reported in
385 the laboratory chamber study (Joseph et al. 2012) (Figure 4B).

386 The observed rapid corrosion and the formation of sulfate as the main corrosion products
387 cannot be explained by either the three-stage corrosion development model (Islander et al. 1991)
388 or the previous theory describing the initiation of corrosion (Jiang et al. 2015b, Joseph et al.
389 2012). The short exposure time suggests that there was likely no development of any sulfide
390 oxidizing microorganisms. Instead, fast chemical oxidation of H_2S to sulfuric acid might be
391 the main cause of the observed fast corrosion and sulfate dominated corrosion products.

392 *3.2. Microbial community in the corrosion layer*

393 To delineate the role of microbes in the observed rapid corrosion, the microbial communities
394 were determined for the combined corrosion layer collected from the four coupons (CA, CB)
395 and from wastewater samples (WA, WB) (**Figure 5)**. In the corrosion layer, *Bacteroides,*
396 *Prevotella 9, Barnesiella, Faecalibacterium, Streptococcus, Christensenellaceae R-7 group,*
397 and *Caulobacter* were detected as the top 8 abundant microbes. Most of these bacteria detected
398 are anaerobes and none of them are known to be capable of oxidizing sulfur. *Bacteroides*
399 *Prevotella 9*, *Barnesiella* and *Faecalibacterium* are obligate anaerobic bacteria, and are found
400 prominently in human guts (Bernhard and Field 2000, Ramirez-Farias et al. 2008, Wu et al.
401 2015). Most *Streptococcus* are facultative anaerobes and are mostly related to infection of
402 human and animals (Cleary et al. 1992). *Firmicutes* are anaerobic microbes and found in
403 various environments including human guts and fuel cell experiments (Ismail et al. 2011,
404 Wrighton et al. 2008). *Christensenellaceae R-7 group* are anaerobic bacteria that can be found
405 in the ruminal mucosa of goats and food waste digester (Jiao et al. 2018, Lee et al. 2017).
406 *Caulobacter* are generally aerobic microbes detected in a dilute aquatic environments with
407 limiting nutrients (Ely 1991). Based on the probable capabilities of these bacteria detected in
408 the oxidative corrosion layers, there is little to suggest they were active components. It is likely
409 we are detecting the remnants of bacteria that have come from the wastewater.

410

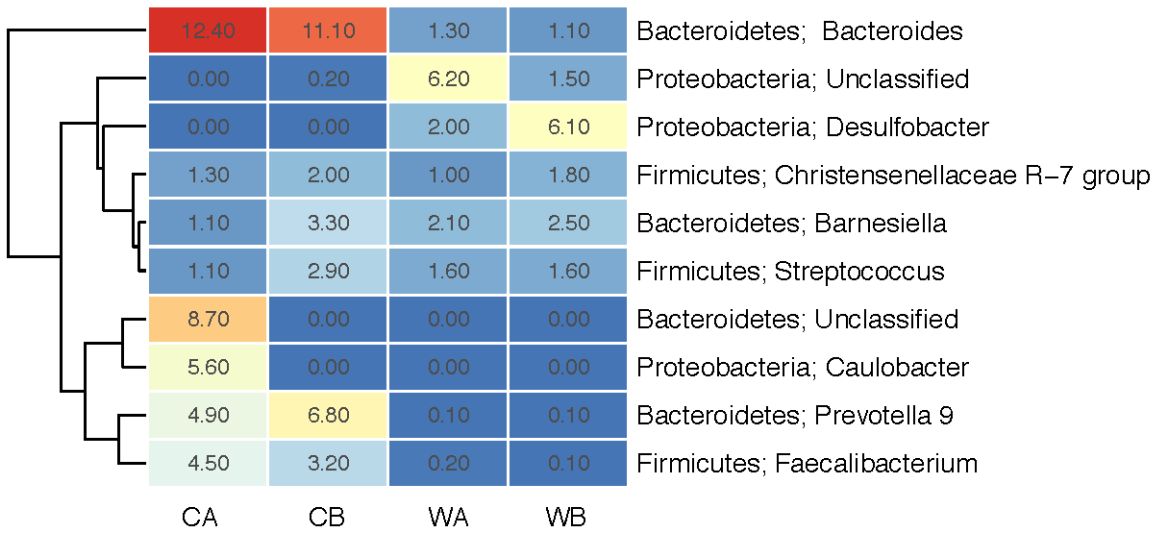

Figure 5. Heatmap summarizing the percent relative abundances of bacteria (each row representing an OTU) in the corrosion layer samples combined from the four coupons (CA and CB). Two wastewater samples from the same sewer pipe was included as WA and WB. Reads that could not be classified are collectively referred to as 'unclassified'.

In microbial induced concrete corrosion, once the pH is reduced to lower than 4, due to the sulfide oxidation and acid production, acidophilic microbes usually become the dominant species (>50%). The most typical genus of acidophilic microorganisms associated with biogenic acid production is *Acidithiobacillus* including *A. ferrooxidans*, *A. thiooxidans*, and *A. caldus* (Davis et al. 1998, Harrison Jr 1984, Islander et al. 1991, Jiang et al. 2016b, Parker 1945b). In addition to *Acidithiobacillus spp.*, *Acidiphilium spp.*, *Mycobacterium spp.*, *Xanthomonadales spp,* are often detected as abundant in acidophilic communities of sewer corrosion layers (Cayford et al. 2017, Jiang et al. 2016b, Li et al. 2017, Okabe et al. 2007, Pagaling et al. 2014). None of these typical acidophilic sulfur-oxidizing microorganisms was detected in the corrosion products collected from the concrete samples in this study. Therefore, it is highly likely that biological sulfide oxidation was not playing a major role in the rapid corrosion observed in the presence of high H_2S levels.

3.3. Sulfide oxidation rates of the concrete coupons after exposure

The SOR of the coupons prior to and after sterilization were quite similar for H_2S concentrations up to 200 ppm (Figure 6). It shows clearly that sterilization of the concrete did not have any impact on the SOR and it confirms that the microbes on the concrete had negligible role in H_2S oxidation. Together with the absence of sulfide oxidizing microbes in the corrosion layer (Section 3.2), it clearly suggests that biological sulfide oxidation is not the cause of the concrete corrosion and thus the SOR observed were mainly due to chemical oxidation of sulfide.

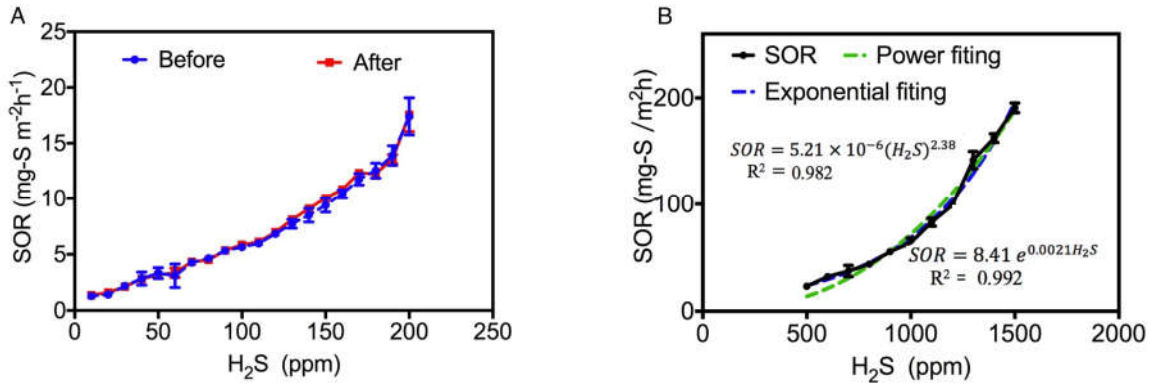

Figure 6. Sulfide oxidation rates of concrete coupons before and after sterilization under 10-200 ppm H_2S (A), and the sulfide oxidation rates of concrete coupons under 500-1500 ppm H_2S (B).

The SOR of both coupons were below 25 mg-S m^{-2} h^{-1} under 10-200 ppm H_2S and increased to around 200 mg-S m^{-2} h^{-1} at approximately 1500 ppm H_2S. The SOR observed for the chemical oxidation process is comparable to the sulfide uptake rate (SUR). SUR is usually used as a good indicator for the development and activity of sulfide oxidizing bacteria in microbial induced concrete corrosion. The SUR of 250 ± 5 mg-S m^{-2} h^{-1} was reported for microbial induced corrosion after 33 months exposure to H_2S at 50 ppm (Sun et al. 2014) and around 100 mg-S m^{-2} h^{-1} for coupons after 17 months exposure under 25 ppm H_2S (Jiang et al. 2016b). At the exposure of 1000 ppm of H_2S, a rapid consumption of H_2S, 3600 mg-S m^{-2} h^{-1} was

449 observed in a pipe section after several months (Vollertsen et al. 2008). Under the same H_2S
450 concentration, the SOR measured in this study was relatively lower compared with previous
451 studies reported for microbially induced corrosion. However, the SOR at above 1000 ppm H_2S
452 of this study were comparable to the uptake rate of microbes under 50 ppm (Sun et al. 2014),
453 which could lead to similar magnitudes of corrosion.

454 Under the high levels of H_2S (500ppm-1500ppm), the SOR increased significantly along with
455 the increase of H_2S concentration (Figure 6B). Kinetic models (i.e. exponential, power), have
456 been previously used to describe the oxidation rate of sulfide in microbially induced concrete
457 corrosion (Æsøy et al. 2002, Sun et al. 2014). Fitting SOR results into exponential kinetics, the
458 exponent showed a positive value (0.0021) (Figure 6B), which is contrary to the negative value
459 previous reported for microbial corrosion (-0.0135) (Sun et al. 2014). In power kinetic models,
460 the reaction order for sulfide oxidation in this study was estimated to be 2.4, which is higher
461 than the reaction order (1.5) previously reported for chemical dominated sulfide oxidation on
462 concrete surfaces and also higher than that reported for microbial induced sulfide oxidation on
463 corroding concrete surfaces (0.45-0.7) (Satoh et al. 2009, Vollertsen et al. 2008). With the
464 highest R^2 (0.995) and lowest sum of residual squares (323.2), exponential kinetics best
465 described the chemical sulfide oxidation on the concrete surface in this study (Table S2). The
466 kinetic analysis suggested that chemical sulfide oxidation is different to the biological sulfide
467 oxidation and that the SOR increases exponentially with H_2S concentration, implicating that
468 chemically induced corrosion will be more severe in sewers with higher H_2S concentrations.

469 *3.4. Chemical oxidation of sulfide in the presence of concrete or corrosion products*

470 In the batch tests with aerated water containing fresh concrete powder, more than 70% of the
471 sulfide was oxidized within 4 hours (Figure 7A) and the total amount of inorganic sulfur species
472 remained constant (Figure S4). The main oxidation products were found to be sulfate and

473 thiosulfate, accounting for 52.6±0.8 % and 42.0±1.3 % of the total oxidized sulfide,
474 respectively. The molar consumption ratio of sulfide to oxygen was 0.8±0.1, which was
475 consistent with the theoretical oxygen demand ratio for the production of sulfate and thiosulfate.
476 During the 4 hour batch tests, the production of elemental sulfur was not observed. The average
477 sulfide oxidation rate was 1.12 ± 0.01 mg-S L^{-1} h^{-1} and the pH was stable at 11.3±0.1 during
478 the whole process. This relatively stable pH is consistent with the strong acid neutralization
479 capacity of concrete powder within the range of pH 13-10 (Figure S3).

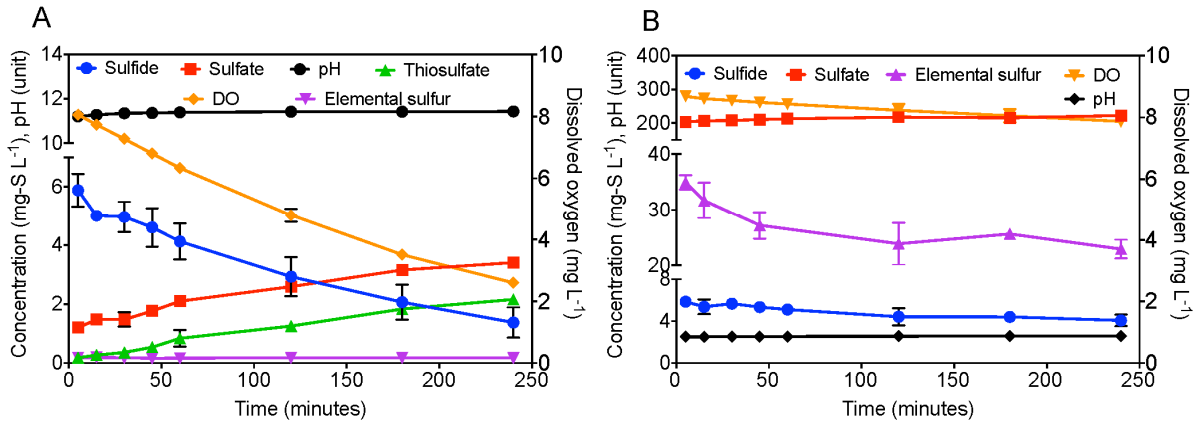

480

481 **Figure 7.** Chemical oxidation of sulfide in aerated water containing fresh concrete powder (A) and
482 autoclaved corrosion layer scrapings (B).

483 For the batch tests containing autoclaved corrosion layer scrapings, 26% of the sulfide dosed
484 was oxidized during the tests (Figure 7B). Along with the sulfate production, the elemental
485 sulfur from the corrosion product was reduced by 35%±5%. The molar consumption ratio of
486 sulfide/oxygen was 1.7±0.1 and the total amount of inorganic sulfur species remained constant.
487 Considering elemental sulfur oxidation and potential formation of polysulfide between
488 elemental sulfur and sulfide, it was unclear whether sulfate production is due to the oxidation
489 of elemental sulfur or sulfide. However, the average sulfide oxidation rate, 0.22±0.02 mg-S L^{-1}
490 h^{-1}, was 5 times lower than the batch tests with fresh concrete powder. Production of sulfite
491 and thiosulfate was not observed over 4 hours and the pH was 2.58±0.09 during the whole

492 process (Figure S4).

493 In previous batch tests, the chemical sulfide oxidation rate in in acidic solutions (pH<2) of
494 suspended corrosion products was reported as 0.01-0.1 mg-S L^{-1} h^{-1} and elemental sulfur was
495 assumed to be the main product as deduced from the oxygen and hydrogen sulfide uptake ratio
496 (Jensen et al. 2011). The chemical sulfide oxidation in solutions of crushed new concrete with
497 high alkalinity has not been reported. For the chemical oxidation of sulfide tests in water,
498 thiosulfate is found as the principal product at pH>8.5, regardless of the sulfide/ oxygen ratio,
499 and the oxidation products were not reported at pH< 6, since the oxidation rate was very slow
500 (Chen and Morris 1972). In this current study, the production of sulfate by chemical oxidation
501 of sulfide in solutions containing either fresh concrete powder or corrosion product was
502 observed and confirmed by direct measurement for the first time. Possibly the reactions
503 observed here are due to metals such as Fe^{2+}, Fe^{3+} and Cu^{2+}, existing in the concrete and
504 corrosion product and catalyzing the chemical oxidation of sulfide. The higher oxidation in
505 fresh concrete solutions suggested more significant impact due to chemical oxidation of sulfide
506 on the concrete corrosion process. Therefore, with sulfuric acid as the main product, chemically
507 induced corrosion of concrete under high H_2S concentration in sewers plays a critical role,
508 especially for newly manufactured concrete sewers.

509 **4. Conclusions**

510 The rapid corrosion of fresh concrete within 20 days at high hydrogen sulfide concentration in
511 sewers was investigated. Different from previous studies, which mainly focus on microbially
512 induced corrosion of concrete sewers, this was the first-ever report of chemically induced
513 corrosion. This has resulted in the following key findings:

514 • Hydrogen sulfide of around 1000 ppm led to fast concrete corrosion within one month,
515 this was characterized by a surface pH around 3 and a corrosion rate around 3 mm $year^{-1}$.

- The fast corrosion of concrete with high levels of H_2S in the sewer was mainly due to the chemical oxidation of hydrogen sulfide to sulfuric acid. No sulfide oxidizing microorganisms were found to participate in the corrosion.
- The rate of chemical sulfide oxidation increased exponentially with hydrogen sulfide concentrations and this could induce potentially high corrosion rates.
- These novel findings of in-sewer corrosion processes hold profound implications for sewer operation and corrosion management. The chemically induced corrosion of newly manufactured concrete sewers would be critical when high H_2S concentrations occur in the sewer atmosphere, especially at certain corrosion hot spots.

Acknowledgements:

The authors acknowledge the financial support provided by the Australian Research Council and the following partners: Gold Coast Water and Waste, District of Columbia Water and Sewer Authority, South East Water for their support through the Australian Research Council Linkage Project LP150101337. Dr Guangming Jiang is the recipient of an Australian Research Council DECRA Fellowship (DE170100694). Xuan Li acknowledges the Chinese Scholarship Council for providing the Living Allowance Scholarship.

Reference:

538 Æsøy, A., Østerhus, S. and Bentzen, G. (2002) Controlled treatment with nitrate in sewers to
539 prevent concrete corrosion. Water Science and Technology: Water Supply 2(4), 137-144.

540 Alexander, M., Bertron, A. and De Belie, N. (2013) Performance of cement-based materials in
541 aggressive aqueous environments, Springer.

542 Australian Standard, A. (1986) 1012.9. Methods for testing concrete.

543 Berndt, M. (2011) Evaluation of coatings, mortars and mix design for protection of concrete
544 against sulphur oxidising bacteria. Construction and Building Materials 25(10), 3893-3902.

545 Bernhard, A.E. and Field, K.G. (2000) A PCR assay to discriminate human and ruminant feces
546 on the basis of host differences in *Bacteroides-Prevotella* genes encoding 16S rRNA. Applied
547 and Environmental Microbiology 66(10), 4571-4574.

548 Cayford, B.I. (2012) Investigation of the microbial community and processes responsible for
549 the corrosion of concrete in sewer systems, University of Queensland, Brisbane.

550 Cayford, B.I., Jiang, G., Keller, J., Tyson, G. and Bond, P.L. (2017) Comparison of microbial
551 communities across sections of a corroding sewer pipe and the effects of wastewater flooding.
552 Biofouling 33(9), 780-792.

553 Chen, K.Y. and Morris, J.C. (1972) Kinetics of oxidation of aqueous sulfide by oxygen.
554 Environmental science & technology 6(6), 529-537.

555 Cleary, P.P., Schlievert, P., Handley, J., Kim, M., Hauser, A., Kaplan, E. and Wlazlo, A. (1992)
556 Clonal basis for resurgence of serious *Streptococcus* pyogenes disease in the 1980s. The Lancet
557 339(8792), 518-521.

558 Davis, J.L., Nica, D., Shields, K. and Roberts, D.J. (1998) Analysis of concrete from corroded
559 sewer pipe. International Biodeterioration & Biodegradation 42(1), 75-84.

560 De Muynck, W., De Belie, N. and Verstraete, W. (2009) Effectiveness of admixtures, surface
561 treatments and antimicrobial compounds against biogenic sulfuric acid corrosion of concrete.
562 Cement and Concrete Composites 31(3), 163-170.

563 Ely, B. (1991) Methods in enzymology, pp. 372-384, Elsevier.

564 Franus, W., Panek, R. and Wdowin, M. (2015) SEM investigation of microstructures in
565 hydration products of portland cement, pp. 105-112, Springer.

566 Grengg, C., Mittermayr, F., Baldermann, A., Böttcher, M., Leis, A., Koraimann, G., Grunert,
567 P. and Dietzel, M. (2015) Microbiologically induced concrete corrosion: A case study from a
568 combined sewer network. Cement and Concrete Research 77, 16-25.

569 Gu, J.-D., Ford, T.E., Berke, N.S. and Mitchell, R. (1998) Biodeterioration of concrete by the
570 fungus *Fusarium*. International Biodeterioration & Biodegradation 41(2), 101-109.

571 Gutierrez-Padilla, M. and Dolores, G. (2007) Activity of Sulfur Oxidizing Microorganisms and
572 impacts on concrete pipe corrosion, University of Colorado at Boulder.

573 Haaning Nielsen, A., Vollertsen, J. and Hvitved-Jacobsen, T. (2004) Chemical sulfide
574 oxidation of wastewater-effects of pH and temperature. Water science and technology 50(4),
575 185-192.

576 Haile, T. and Nakhla, G. (2010) The inhibitory effect of antimicrobial zeolite on the biofilm of
577 Acidithiobacillus thiooxidans. Biodegradation 21(1), 123-134.

578 Harrison Jr, A.P. (1984) The acidophilic thiobacilli and other acidophilic bacteria that share
579 their habitat. Annual Reviews in Microbiology 38(1), 265-292.

Hvitved-Jacobsen, T., Vollertsen, J. and Nielsen, A.H. (2013) Sewer processes: microbial and chemical process engineering of sewer networks, CRC press.

Islander, R.L., Devinny, J.S., Mansfeld, F., Postyn, A. and Shih, H. (1991) Microbial ecology of crown corrosion in sewers. Journal of Environmental Engineering 117(6), 751-770.

Ismail, N.A., Ragab, S.H., ElBaky, A.A., Shoeib, A.R., Alhosary, Y. and Fekry, D. (2011) Frequency of *Firmicutes and Bacteroidetes* in gut microbiota in obese and normal weight Egyptian children and adults. Archives of medical science: AMS 7(3), 501.

Jana, D. and Lewis, R.A. (2005) Acid attack in a concrete sewer pipe–a petrographic and chemical investigation.

Jensen, H.S., Lens, P.N., Nielsen, J.L., Bester, K., Nielsen, A.H., Hvitved-Jacobsen, T. and Vollertsen, J. (2011) Growth kinetics of hydrogen sulfide oxidizing bacteria in corroded concrete from sewers. Journal of hazardous materials 189(3), 685-691.

Jensen, H.S., Nielsen, A.H., Hvitved-Jacobsen, T. and Vollertsen, J. (2009) Modeling of hydrogen sulfide oxidation in concrete corrosion products from sewer pipes. Water Environment Research 81(4), 365-373.

Jiang, G., Keller, J. and Bond, P.L. (2014) Determining the long-term effects of H_2S concentration, relative humidity and air temperature on concrete sewer corrosion. Water Res 65, 157-169.

Jiang, G., Keller, J., Bond, P.L. and Yuan, Z. (2016a) Predicting concrete corrosion of sewers using artificial neural network. Water Res 92, 52-60.

Jiang, G., Melder, D., Keller, J. and Yuan, Z. (2017) Odor emissions from domestic wastewater: A review. Critical Reviews in Environmental Science and Technology 47(17), 1581-1611.

Jiang, G., Sharma, K.R., Guisasola, A., Keller, J. and Yuan, Z. (2009) Sulfur transformation in rising main sewers receiving nitrate dosage. Water Research 43(17), 4430-4440.

Jiang, G., Sun, J., Sharma, K.R. and Yuan, Z. (2015a) Corrosion and odor management in sewer systems. Current Opinion in Biotechnology 33, 192-197.

Jiang, G., Sun, X., Keller, J. and Bond, P.L. (2015b) Identification of controlling factors for the initiation of corrosion of fresh concrete sewers. Water Research 80, 30-40.

Jiang, G., Zhou, M., Chiu, T.H., Sun, X., Keller, J. and Bond, P.L. (2016b) Wastewater Enhanced Microbial Corrosion of Concrete Sewers. Environ Sci Technol.

Jiao, J., Wu, J., Wang, M., Zhou, C., Zhong, R. and Tan, Z. (2018) Rhubarb supplementation promotes intestinal mucosal innate immune homeostasis through modulating intestinal epithelial microbiota in goat kids. Journal of agricultural and food chemistry 66(4), 1047-1057.

Joseph, A.P., Keller, J., Bustamante, H. and Bond, P.L. (2012) Surface neutralization and H_2S oxidation at early stages of sewer corrosion: influence of temperature, relative humidity and H_2S concentration. Water Research 46(13), 4235-4245.

Keller-Lehmann, B., Corrie, S., Ravn, R., Yuan, Z. and Keller, J. (2006) Preservation and simultaneous analysis of relevant soluble sulfur species in sewage samples, p. 28.

Kutchko, B.G. and Kim, A.G. (2006) Fly ash characterization by SEM–EDS. Fuel 85(17-18), 2537-2544.

Lahav, O., Lu, Y., Shavit, U. and Loewenthal, R.E. (2004) Modeling hydrogen sulfide emission rates in gravity sewage collection systems. Journal of Environmental Engineering 130(11), 1382-1389.

Lee, J., Shin, S.G., Han, G., Koo, T. and Hwang, S. (2017) Bacteria and archaea communities in full-scale thermophilic and mesophilic anaerobic digesters treating food wastewater: Key process parameters and microbial indicators of process instability. Bioresource technology 245, 689-697.

Li, X., Jiang, G., Kappler, U. and Bond, P. (2017) The ecology of acidophilic microorganisms in the corroding concrete sewer environment. Frontiers in microbiology 8, 683.

Mori, T., Koga, M., Hikosaka, Y., Nonaka, T., Mishina, F., Sakai, Y. and Koizumi, J. (1991) Microbial corrosion of concrete sewer pipes, H2S production from sediments and determination of corrosion rate. Water science and technology 23(7-9), 1275-1282.

Nica, D., Davis, J.L., Kirby, L., Zuo, G. and Roberts, D.J. (2000) Isolation and characterization of microorganisms involved in the biodeterioration of concrete in sewers. International Biodeterioration & Biodegradation 46(1), 61-68.

Okabe, S., Odagiri, M., Ito, T. and Satoh, H. (2007) Succession of sulfur-oxidizing bacteria in the microbial community on corroding concrete in sewer systems. Appl Environ Microbiol 73(3), 971-980.

Pagaling, E., Yang, K. and Yan, T. (2014) Pyrosequencing reveals correlations between extremely acidophilic bacterial communities with hydrogen sulphide concentrations, pH and inert polymer coatings at concrete sewer crown surfaces. J Appl Microbiol 117(1), 50-64.

Parker, C. (1945a) The corrosion of concrete 2. The function of *Thiobacillus concretivorus* (nov. spec.) in the corrosion of concrete exposed to atmospheres containing hydrogen sulphide. Australian Journal of Experimental Biology & Medical Science 23(2).

Parker, C.D. (1945b) The corrosion of concrete. Aust J Exp Biol Med 23(2), 81-90.

Parker, C.t. (1947) Species of sulphur bacteria associated with the corrosion of concrete. Nature 159(4039), 439-440.

Ramirez-Farias, C., Slezak, K., Fuller, Z., Duncan, A., Holtrop, G. and Louis, P. (2008) Effect of inulin on the human gut microbiota: stimulation of *Bifidobacterium adolescentis* and *Faecalibacterium prausnitzii*. British Journal of Nutrition 101(4), 541-550.

Satoh, H., Odagiri, M., Ito, T. and Okabe, S. (2009) Microbial community structures and in situ sulfate-reducing and sulfur-oxidizing activities in biofilms developed on mortar specimens in a corroded sewer system. Water Research 43(18), 4729-4739.

Sharma, K.R., Yuan, Z., de Haas, D., Hamilton, G., Corrie, S. and Keller, J. (2008) Dynamics and dynamic modelling of H_2S production in sewer systems. Water Research 42(10-11), 2527-2538.

Song, Y., Tian, Y., Li, X., Wei, J., Zhang, H., Bond, P.L., Yuan, Z. and Jiang, G. (2018a) Distinct microbially induced concrete corrosion at the tidal region of reinforced concrete sewers. Water Research.

Song, Y., Wightman, E., Tian, Y., Jack, K., Li, X., Zhong, H., Bond, P.L., Yuan, Z. and Jiang, G. (2018b) Corrosion of reinforcing steel in concrete sewers. Science of the total environment.

Standard AS2972, A. 3972. 2010. General Purpose and Blended Cements.

Sun, X., Jiang, G., Bond, P.L., Keller, J. and Yuan, Z. (2015) A novel and simple treatment for control of sulfide induced sewer concrete corrosion using free nitrous acid. Water Res 70, 279-287.

665 Sun, X., Jiang, G., Bond, P.L., Wells, T. and Keller, J. (2014) A rapid, non-destructive
666 methodology to monitor activity of sulfide-induced corrosion of concrete based on H 2 S
667 uptake rate. Water Research 59, 229-238.

668 Vollertsen, J., Nielsen, A.H., Jensen, H.S., Wium-Andersen, T. and Hvitved-Jacobsen, T.
669 (2008) Corrosion of concrete sewers—the kinetics of hydrogen sulfide oxidation. Science of
670 the total environment 394(1), 162-170.

671 Wells, T. and Melchers, R.E. (2015) Modelling concrete deterioration in sewers using theory
672 and field observations. Cement and Concrete Research 77, 82-96.

673 Wells, T., Melchers, R.E. and Bond, P. (2009) Factors involved in the long term corrosion of
674 concrete sewers. Australasian corrosion association proceedings of corrosion and prevention,
675 Coffs Harbour, Australia 11.

676 Wrighton, K.C., Agbo, P., Warnecke, F., Weber, K.A., Brodie, E.L., DeSantis, T.Z.,
677 Hugenholtz, P., Andersen, G.L. and Coates, J.D. (2008) A novel ecological role of the
678 *Firmicutes* identified in thermophilic microbial fuel cells. The ISME journal 2(11), 1146.

679 Wu, M., McNulty, N.P., Rodionov, D.A., Khoroshkin, M.S., Griffin, N.W., Cheng, J., Latreille,
680 P., Kerstetter, R.A., Terrapon, N. and Henrissat, B. (2015) Genetic determinants of in vivo
681 fitness and diet responsiveness in multiple human gut *Bacteroides*. Science 350(6256),
682 aac5992.

683 Zhang, L., De Schryver, P., De Gusseme, B., De Muynck, W., Boon, N. and Verstraete, W.
684 (2008) Chemical and biological technologies for hydrogen sulfide emission control in sewer
685 systems: A review. Water Research 42(1–2), 1-12.

686